Beware of Temperature Increase During Rapid Vessel Charging

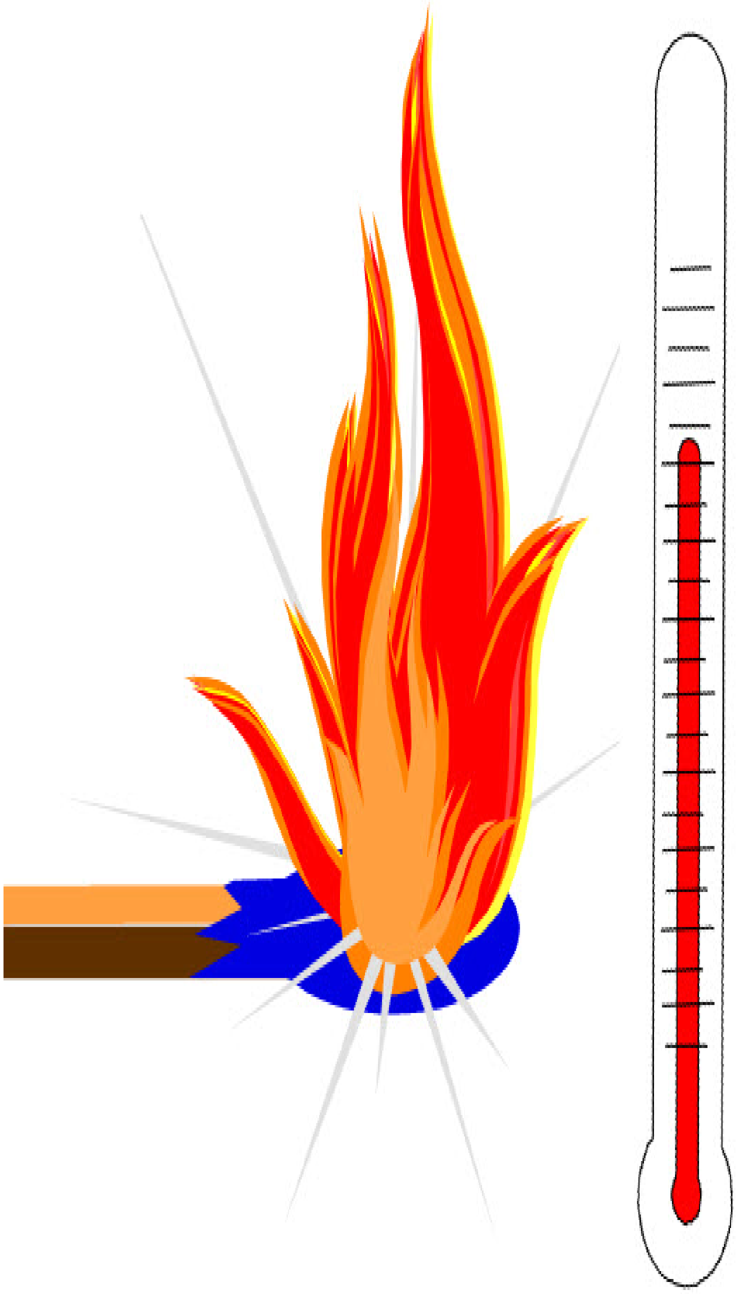

An ioMosaic® Publication

G. A. Melhem, Ph.D., FAIChE

ioMosaic® Corporation

Beware of Temperature Increase During Rapid Vessel Charging

Process Safety and Risk Management Practices

authored by

G. A. Melhem, Ph.D., FAIChE

Printed October 24, 2024

Notice:

Revision Log:

Revision 1: March 15, 2022

...

Table of Contents

1 Introduction 5

2 Multiphase Generalized Mass and Energy Balances 5

3 Vessels Containing Non-Ideal Gas 8

4 Simplified Generalized Mass and Energy Balances 9

5 Simplified Ideal Gas Generalized Mass and Energy Balances 11

6 Ideal Gas Vessel Charging 12

7 Pressure Relief Systems Considerations 14

8 Temperature Increase Caused by Bubble Compression 15

9 Compression Ignition 19

10 Conclusions 20

A Appendix A - Volume Change for Piping and Vessels ($\frac{dV_s}{dt}$) 21
- A.1 Change of Volume with Respect to Temperature 21
- A.2 Change of Volume with Respect to Pressure 22
- A.3 Volume Change for Fluids 23

B Appendix B - Ideal Nozzle Flow Rates 24
- B.1 Liquids 24
- B.2 Ideal Gases 24

List of Figures

1 SuperChems Expert prediction of pressure during vessel charging using non-ideal gas behavior 14
2 SuperChems Expert prediction of temperature during vessel charging using non-ideal gas behavior 15
3 SuperChems Expert Venting dynamics from high pressure separator into low pressure receiver - Pressure 16
4 SuperChems Expert Venting dynamics from high pressure separator into low pressure receiver - Temperature 16
5 Temperature dependency of modulus of elasticity for some common materials of construction [1] 22

List of Tables

1 Vessel Charging Parameters 12

2 The Interface Temperature (C) Driven at Adiabatic Bubble Compressions 19

3 Compressed Temperature as a function of pressure 20

4 Coefficient of linear thermal expansion for some common metals and materials of construction at 293.15 K 23

1 Introduction

The rapid introduction of a fluid from a high pressure source into a lower pressure receiver can result in rapid heating of the mixed fluid in the receiver. The extent of temperature rise will depend on the initial conditions of the source and receiver fluids including temperature, pressure, composition, phase, and the rate of mass inflow.

For the special case of ideal gas inflow from a high pressure source into a low pressure receiver that also contains an ideal gas, we can demonstrate from first principles that the final temperature will asymptote to γT_o, where T_o is the high pressure source fluid temperature. This condition is encountered for example when compressed natural gas vehicles are filled, or when a high pressure gas is introduced into a downstream receiver due to the failure of a heat exchanger tube or control valve.

When introduction of mass and energy into the receiver vessel occurs rapidly, heat exchange between the fluid, vessel walls, and the surroundings becomes negligible. This can lead to high fluid temperatures that may cause material of construction problems, and/or cause the decomposition of chemicals or mixtures containing ethylene or other reactive components. Slower introduction of mass and energy into the receiver allows for more heat exchange with the vessel walls and surroundings resulting in lower peak fluid temperatures. We also discuss the potential for compression ignition and the increase in temperature that can be caused by spontaneous bubble compression.

We first develop the overall fundamental mass and energy balances for a non-ideal, multi-phase constant volume system to illustrate how mass and energy can be added or depleted from a constant volume system. We then simplify these general balances to represent a single gas phase with non-ideal behavior. We further simplify the single phase balances using ideal gas behavior to derive the fluid temperature asymptote of γT_o. This asymptote provides a simple screening criteria.

2 Multiphase Generalized Mass and Energy Balances

Consider a vessel containing a reacting two-phase multicomponent mixture of total volume V, temperature T, and pressure P. It is assumed that both the vapor and liquid phases are always in thermal, mechanical, and diffusional equilibrium. The vapor and liquid phases are considered to be homogeneous in composition and state. When a change of phase is exhibited, mass may be transferred from one phase to the other. Thus, the state of either phase may be altered by a change in composition, temperature, or pressure.

The value of any thermodynamic property, M, in either phase may be expressed as a function of temperature, pressure, and number of moles of the individual mixture components:

$$M = f(T, P, z_1, z_2, \cdots, z_C) \tag{1}$$

where z_i is the number of moles of species i in the mixture and C is the total number of components.

We can write an equation for a differential change in property M during a small change in phase:

$$dM = \left(\frac{\partial M}{\partial P}\right)_{T,z_1,z_2,\cdots} dP + \left(\frac{\partial M}{\partial T}\right)_{P,z_1,z_2,\cdots} dT + \sum_i^C \left(\frac{\partial M}{\partial z_i}\right)_{T,P,z_{j\neq i}} dz_i \tag{2}$$

This differential statement of Equation 1 is extended to permit calculation of the change of property, M, with respect to any other system variable, e.g. time, t:

$$\frac{dM}{dt} = \left(\frac{\partial M}{\partial P}\right)_{T,z_1,z_2,\cdots} \frac{dP}{dt} + \left(\frac{\partial M}{\partial T}\right)_{P,z_1,z_2,\cdots} \frac{dT}{dt} + \sum_i^C \left(\frac{\partial M}{\partial n_i}\right)_{T,P,z_{j\neq i}} \frac{dz_i}{dt} \tag{3}$$

The partial derivatives of thermodynamic properties necessary for equilibrium, and fluid flow calculations are obtained from a suitable equation of state [2, 3].

Neglecting potential energy effects, the unsteady behavior of the system can be completely described based on first principles by writing the equations describing the internal energy change, the constant volume constraint, conservation of mass, and vapor-liquid equilibrium relations [4].

The overall internal energy change of the system is:

$$\begin{aligned}
&\left[N_{\text{internals}} C_{v_{\text{internals}}} + \sum_i^C (N_i + n_i) C_{v_i} + N_T \frac{\partial \Delta \underline{U}_v}{\partial T} + n_T \frac{\partial \Delta \underline{U}_l}{\partial T}\right] \frac{dT}{dt} \quad + \\
&\qquad \left[N_T \frac{\partial \Delta \underline{U}_v}{\partial P} + n_T \frac{\partial \Delta \underline{U}_l}{\partial P}\right] \frac{dP}{dt} \quad + \\
&\qquad \sum_i^C \left(\underline{U}_{i,ref} + \int_{T_{ref}}^{T} C_{v_i} dT + \Delta \underline{U}_v + N_T \frac{\partial \Delta \underline{U}_v}{\partial N_i}\right) \frac{dN_i}{dt} \quad + \\
&\qquad \sum_i^C \left(\underline{U}_{i,ref} + \int_{T_{ref}}^{T} C_{v_j} dT + \Delta \underline{U}_l + n_T \frac{\partial \Delta \underline{U}_l}{\partial n_i}\right) \frac{dn_i}{dt} \quad = \\
&\dot{Q} + \dot{H}_{l,in} + \dot{E}_{l,in} + \dot{H}_{v,in} + \dot{E}_{v,in} - \dot{H}_{l,out} - \dot{E}_{l,out} - \dot{H}_{v,out} - \dot{E}_{v,out}
\end{aligned} \tag{4}$$

Here $\dot{Q}$ represents the rate of heat gained/lost by the vessel contents from/to the surroundings including fire loading and convective/conductive heat transfer. Although Equation 4 is used by SuperChems Expert$^{\text{TM}}$ to model the unsteady flow dynamics of vessels containing multiphase systems, $\dot{Q}$ is calculated in a more complete fashion by segmenting the vessel wall into multiple zones and enabling a wide variety of heat transfer mechanisms and options such as fire exposure, rain cooling, water sprays, insulation, etc. (see [5, 6]). $\Delta \underline{U}$ represents the internal energy departure from ideality function, N represents the number of moles in the vapor phase, n represents the number of moles in the liquid phase, $\underline{U}$ represents the molar internal energy, C_v the molar non-ideal heat capacity at constant volume, $\dot{H}$ is the total enthalpy flow in and out of the system, $\dot{E}$ is the kinetic energy flow in and out of the system, $_T$ represents a total quantity, $_i$ represents a species i property, $_v$ represents a vapor/gas phase property, $_l$ represents a liquid phase property, $_{in}$

represents an input to the system, $_{out}$ represents an output from the system, $_s$ represents a vessel property, and $\underline{U}_{i,ref}$ is the internal energy of formation of species i. The heat effects of any internal vessel components are accounted for by the $N_{\text{internals}} C_{v_{\text{internals}}}$ term in Equation 4. It is interesting to note that the heat of reaction for any given reaction is implicitly added or removed from the system when the individual number of moles are changed.

The constant volume constraint is expressed as follows:

$$\frac{dV_s}{dt} = (V_v\beta_v + V_l\beta_l)\frac{dT}{dt} - (V_v\kappa_v + V_l\kappa_l)\frac{dP}{dt} + \sum_i \overline{V}_{v_i}\frac{dN_i}{dt} + \sum_i \overline{V}_{l_i}\frac{dn_i}{dt} \tag{5}$$

where $\frac{dV_s}{dt}$ is the change of vessel metal volume due to temperature and internal pressure changes, normally set to 0 (see Appendix A), $\overline{V}$ is the partial molar volume, κ is the isothermal compressibility, and β is the volume expansion coefficient.

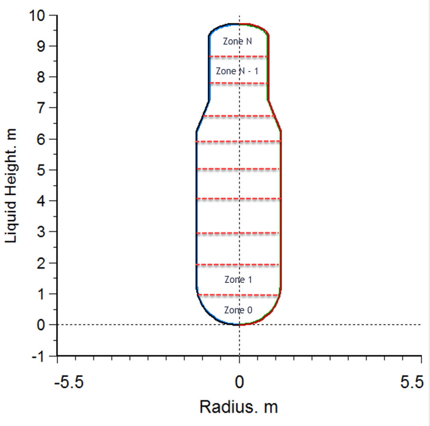

The conservation of mass equations are:

$$\frac{dn_i}{dt} + \frac{dN_i}{dt} = \dot{n}_{i,in} + \dot{N}_{i,in} - \dot{n}_{i,out} - \dot{N}_{i,out} + \dot{R}_i \quad (\text{for } i = 1, \cdots, C) \tag{6}$$

where $\dot{R}_i$ is the overall production rate of species i for all chemical reactions involving the ith species, $\dot{n}_i$ is the liquid molar flow rate of species i and $\dot{N}_i$ is the vapor molar flow rate of species i.

The equilibrium relations between the vapor and the liquid phases are written as functions of the liquid and vapor fugacity coefficients, $\hat{\phi}$:

$$\frac{N_i}{N_T} - \frac{n_i}{n_T}\frac{\hat{\phi}_{l,i}}{\hat{\phi}_{v,i}} = 0 \quad (\text{for } i = 1, \cdots, C) \tag{7}$$

For ideal systems, Equation 7 can be rewritten as a function of the species saturation pressures:

$$\frac{N_i}{N_T} - \frac{n_i}{n_T}\frac{P_{sat,i}}{P} = 0 \quad (\text{for } i = 1, \cdots, C) \tag{8}$$

where P_{sat} is the vapor pressure.

Vapor, gassy and hybrid system behaviors are all described by Equations 7 and 8, which determine the distribution of reaction reactants and products between the liquid and vapor phases.

Equations 4, 5, 6, and 7 yield $2C + 2$ differential algebraic equations. These equations are solved by SuperChems using a sparse implementation of the semi-implicit Runge-Kutta algorithm of Michelsen [7]. This algorithm is applicable to the solution of simultaneous differential and non-linear algebraic equations to include stiff systems. The individual molar flow rates, $\dot{n}_i$ and $\dot{N}_i$, are determined at each time increment for either nozzle or pipe flow using available single and multiphase flow methods in SuperChems .

3 Vessels Containing Non-Ideal Gas

The generalized equations for multiphase energy and mass balances can be simplified for the special case where a single gas/vapor phase is present. We assume that the vessel still contains a multicomponent vapor mixture. The unsteady behavior of the system can be completely described based on first principles by writing the single phase equations describing the internal energy change [1], the constant volume constraint, and conservation of mass. Phase equilibrium relations are no longer needed. It can be shown that the overall internal energy change of the system is represented by one equation relating the overall temperature and pressure changes:

$$a\frac{dT}{dt} + b\frac{dP}{dt} = c \tag{9}$$

where a, b, and c are constants defined as follows:

$$\begin{aligned}
a &= N_{\text{internals}} C_{v_{\text{internals}}} + \sum_i^C N_i C_{v_i} + N_T \frac{\partial \Delta \underline{U}_v}{\partial T} \\
b &= N_T \frac{\partial \Delta \underline{U}_v}{\partial P} \\
c &= \dot{Q} + \dot{H}_{v,in} + \dot{E}_{v,in} - \dot{H}_{v,out} - \dot{E}_{v,out} - \sum_i^C \left(\underline{U}_{i,ref} + \int_{T_{\text{ref}}}^{T} C_{v_i} dT + \Delta \underline{U}_v + N_T \frac{\partial \Delta U_v}{\partial N_i} \right) \frac{dN_i}{dt}
\end{aligned}$$

To reduce the internal pressure for vessels containing vapor exposed to fire or external heating, vapor must be removed at a sufficient rate to offset the change in density of the vessel vapor during pressure reduction.

The constant volume constraint is expressed as follows:

$$\beta_v \frac{dT}{dt} - \kappa_v \frac{dP}{dt} - 3\alpha_s \frac{dT}{dt} - \left(\frac{D_i}{\delta}\right)\left(\frac{1}{E_{s,T}}\right) f(\nu) \frac{dP}{dt} = \underbrace{-\frac{1}{V_v} \sum_i \overline{V}_{v_i} \frac{dN_i}{dt}}_{d} \tag{10}$$

where α_s is the material of construction coefficient of thermal linear expansion, $E_{s,T}$ is the material of construction modulus of elasticity, D_i is the internal vessel diameter, δ is the vessel wall thickness, ν is Poisson's ratio, and $f(\nu)$ depends on the vessel geometry (see Appendix A):

$$f(\nu) = 1.25 - \nu \simeq 0.95 \quad \text{for a cylindrical vessel, and} \tag{11}$$

$$f(\nu) = \frac{3}{4}(1 - \nu) \simeq 0.53 \quad \text{for spherical vessel.} \tag{12}$$

The conservation of mass equations are:

$$\frac{dN_i}{dt} = \dot{N}_{i,in} - \dot{N}_{i,out} + \dot{R}_i \quad (\text{for } i = 1, \cdots, C) \tag{13}$$

---

[1] Use of enthalpy is incorrect since this is a constant volume system.

Equations 9, 10 and 13 yield $C+2$ ordinary differential equations. The individual molar flow rates $\dot{N}_i$ are determined at each time increment using a variety of SuperChems nozzle and/or pipe flow options.

Equations 9, 10 and 13 can be solved directly for the change in temperature and pressure as a function of time including the vessel metal change in volume:

$$\frac{dP}{dt} = \frac{c\left(\beta_v - 3\alpha_s\right) - da}{b\left(\beta_v - 3\alpha_s\right) + \left[\kappa_v + \left(\frac{D_i}{\delta}\right)\left(\frac{1}{E_{s,T}}\right) f(\nu)\right] a} \tag{14}$$

$$\frac{dT}{dt} = \frac{c}{a} - \frac{b}{a}\frac{dP}{dt} \tag{15}$$

The above single phase equations (13, 14, and 15) are also solved dynamically by SuperChems using a sparse implementation of the semi-implicit Runge-Kutta algorithm of Michelsen [7].

4 Simplified Generalized Mass and Energy Balances

We can further simplify the single phase equations above to provide working equations for a non-ideal fluid with one component and one phase. Simplifying the detailed vessel balances derived above and ignoring the fluid partial molar volumetric change, we can fully describe the temperature and pressure changes for the fluid in the vessel:

Mass Balance:

$$\frac{dm}{dt} = \dot{m}_{in} - \dot{m}_{out} \tag{16}$$

Internal Energy Balance:

$$\left(mc_v + m_s c_{v,s}\right)\frac{dT}{dt} + U\frac{dm}{dt} = \dot{Q} - \dot{H}_{out} - \dot{E}_{out} + \dot{H}_{in} + \dot{E}_{in} \tag{17}$$

or

$$\frac{dT}{dt} = \frac{\dot{Q} + \dot{H}_{in} + \dot{E}_{in} - \dot{H}_{out} - \dot{E}_{out} - U\frac{dm}{dt}}{mc_v + m_s c_{v,s}} \tag{18}$$

and

$$c_v = c_p - \frac{T\beta^2}{\rho\kappa} \tag{19}$$

where U is the specific internal energy, ρ is the mass density, m is the mass of the fluid, c_v and c_p are the non-ideal fluid specific heat capacities at constant volume and pressure respectively.

Expressing internal energy and enthalpy in terms of c_p and c_v leads to the following expression for dT/dt:

$$\frac{dT}{dt} = \frac{\dot{Q} + \underbrace{\frac{1}{2}\left(\dot{m}_{in}u_{in}^2 - \dot{m}_{out}u_{out}^2\right)}_{\dot{E}_{in}-\dot{E}_{out}} + \left(\dot{m}_{in} - \dot{m}_{out}\right)q - \dot{m}_{in}q* + \dot{m}_{in}q^{'}}{m\left[c_p - \frac{T\beta^2}{\rho\kappa}\right] + m_s c_{v,s}} \tag{20}$$

$$q = \int_{T_0}^{T}\left(c_p - c_v\right)dT = \int_{T_0}^{T}\left[\frac{T\beta^2}{\rho\kappa}\right]dT \tag{21}$$

$$q^* = \int_{T_0}^{T} c_p dT \tag{22}$$

$$q^{'} = \int_{T_0}^{T_{in}} c_p dT \tag{23}$$

$$\frac{dq}{dt} = c_p - c_v = \frac{T\beta^2}{\rho\kappa} \tag{24}$$

$$\frac{dq^*}{dt} = c_p \tag{25}$$

where u is the flow velocity. For liquid full systems, the internal energy equation assumes that the vessel material of construction is at the same temperature as the fluid because the heat transfer coefficient between the inner wall of the vessel and the fluid is large enough. This is only a reasonable approximation for liquid full vessels. Detailed analysis involving actual heat transfer through the metal shows that for gas filled vessels the metal will heat up much faster than the gas contents [5, 6] under external heating and/or fire exposure.

Overall Volume Balance:

$$V = \frac{m}{\rho} \tag{26}$$

$$\frac{dV_{excess}}{dt} = V\beta\frac{dT}{dt} - V\kappa\frac{dP}{dt} - 3\alpha_s V_s\frac{dT}{dt} - \left(\frac{D_i}{\delta}\right)\left(\frac{V_s}{E_{s,T}}\right)f(\nu)\frac{dP}{dt} = 0 \tag{27}$$

or since V_s must equal V at all times:

$$\frac{dP}{dt} = \left[\frac{V\beta - 3\alpha_s V_s}{V\kappa + \left(\frac{D_i}{\delta}\right)\left(\frac{V_s}{E_{s,T}}\right)f(\nu)}\right]\frac{dT}{dt} = \left[\frac{\left(\beta - 3\alpha_s\right)E_{s,T}}{E_{s,T}\kappa + \left(\frac{D_i}{\delta}\right)f(\nu)}\right]\frac{dT}{dt} \tag{28}$$

Vessel Metal Volume:

$$\frac{dV_s}{dt} = 3\alpha_s V_s\frac{dT}{dt} + \left(\frac{D_i}{\delta}\right)\left(\frac{V_s}{E_{s,T}}\right)f(\nu)\frac{dP}{dt} \tag{29}$$

PVT:

$$\rho = f\left(T, P\right) = \frac{m}{V} = \frac{m}{V_s} \tag{30}$$

The above equations can easily be solved using a differential equations solver for T, P, V_s, and V as a function of time. For liquid full vessels, the solution is valid until the temperature of liquid equals the bubble point temperature at the calculated pressure at which point a two-phase solution is required. The solution requires temperature dependent values of thermodynamic properties. The values of β and κ are almost always obtained from an equation of state [2, 3] or actual measured data. The constant volume heat capacity of the vessel material of construction is effectively equal to the heat capacity at constant pressure.

5 Simplified Ideal Gas Generalized Mass and Energy Balances

For a single phase ideal gas fluid, we can show that gas pressure, temperature, and mass change as a function of time as follows:

$$\frac{dm}{dt} = \dot{m}_{in} - \dot{m}_{out} \tag{31}$$

$$\frac{dT}{dt} = \frac{1}{mc_v + m_s c_{v,s}}\left[\dot{Q} + \frac{\left(\dot{m}_{in}u_{in}^2 - \dot{m}_{out}u_{out}^2\right)}{2} + c_v\gamma\left(\dot{m}_{in}T_{in} - \dot{m}_{out}T\right) - c_vT\frac{dm}{dt}\right] \tag{32}$$

$$\frac{dP}{dt} = \frac{R_g}{M_wV}\left[T\frac{dm}{dt} + m\frac{dT}{dt}\right] \tag{33}$$

$$\frac{dV}{dt} = \frac{dV_s}{dt} = 3\alpha_s\frac{dT}{dt} + \left(\frac{D_i}{\delta}\right)\left(\frac{1}{E_{s,T}}\right)f(\nu)\frac{dP}{dt} \tag{34}$$

$$\rho = \frac{m}{V} = \frac{PM_w}{R_gT} \tag{35}$$

where c_vT is the specific internal energy of the gas, $c_v\gamma T$ is the specific enthalpy of the gas, $\dot{m}_i$ is the mass flow into the vessel at temperature T_i, $\dot{m}_o$ is the mass flow out of the vessel at the gas temperature T, $c_v = \frac{R_g}{M_w(\gamma-1)}$ is the specific heat capacity at constant volume, R_g is the universal gas constant, $\dot{Q}$ is the heat exchange rate between the gas and vessel metal and/or surroundings, γ is the ideal gas heat capacity ratio, m is the gas total mass, ρ is the gas mass density, and V is the total volume. The subscript $_s$ references the vessel material of construction where α_s is the material of construction coefficient of thermal linear expansion, $E_{s,T}$ is the material of construction modulus of elasticity, D_i is the internal vessel diameter, δ is the vessel wall thickness, ν is Poisson's ratio, and $f(\nu)$ depends on the vessel geometry. If we ignore vessel metal expansion and/or contraction, then:

$$\frac{dV}{dt} = \frac{dV_s}{dt} = 0 \tag{36}$$

These equations can be used to calculate the temperature, pressure, and mass time histories during a vessel blowdown, or during charging of a gas vessel. These equations assume that the vessel metal is at the same temperature as the vessel contents. Detailed analysis involving actual heat transfer through the metal shows that for gas filled vessels the metal will heat up much faster than the gas contents [5] under external heating or fire exposure.

6 Ideal Gas Vessel Charging

As a final simplification of the ideal gas equations described above, we neglect heat exchange and only consider mass inflow into the system. As an illustration, we consider the constant adiabatic flow of an ideal gas from a large reservoir into a small receiver through a 1 inch ideal connection where the nozzle discharge coefficient is equal to 1, $C_d = 1$. This example simulates the gas blow through from a high pressure separator into the vapor space of a kerosene stripper due the failure of a control valve. The high pressure gas separator fluid molar composition is 81.02 $\%$ hydrogen, 11.98 $\%$ methane, 3.82 $\%$ ethane, 1.74 $\%$ propane, and 1.44 $\%$ butane. The detailed equations presented above are simplified to determine the time history of temperature, pressure, and mass in the small volume.

Table 1: Vessel Charging Parameters

Variable	Value
Reservoir Volume, V_o	10 m^3
Reservoir Pressure, P_o	4000 kPag
Reservoir Temperature, T_o	210 C
Molecular Weight, M_w	6.30
Heat Capacity Ratio, γ	1.302
Initial Flow Rate, $\dot{m}_o$	1.282 kg/s
Receiver Volume, V	1.93 m^3
Receiver Initial Mass, M_i	1.64 kg
Receiver Initial Pressure, P_i	448 kPag
Receiver Initial Temperature, T_i	210 C

Three balances can be written for the receiver, an internal energy balance, a mass balance, and a constant volume balance.

Internal Energy

$$\frac{d}{dt}\left[MU\right] = +\dot{m}_o H_o \tag{37}$$

$$U = \frac{R_g T}{M_w\left(\gamma - 1\right)} \tag{38}$$

$$H_o = \frac{R_g T_o}{M_w}\frac{\gamma}{\left(\gamma - 1\right)} \tag{39}$$

$$\frac{dT}{dt} = \frac{\dot{m}_o}{M}\left[\gamma T_o - T\right] \tag{40}$$

where M is the total gas mass, $\dot{m}_o$ is the mass flow into the receiver, H_o is the specific enthalpy of the incoming flow into the receiver, M_w is the average molecular weight, γ is the ideal gas heat capacity ratio, R_g is the universal gas constant, and T_o is the temperature of the incoming fluid into the receiver.

Mass

$$\frac{dM}{dt} = +\dot{m}_o \tag{41}$$

Constant Volume

$$\frac{dV}{dt} = 0 \tag{42}$$

$$\frac{1}{T}\frac{dT}{dt} - \frac{1}{P}\frac{dP}{dt} = -\frac{1}{M}\frac{dM}{dt} \tag{43}$$

$$\frac{dP}{dt} = \frac{R_g M}{M_w V}\left[\frac{dT}{dt} + \frac{\dot{m}_o}{M}T\right] \tag{44}$$

Integrating the mass and internal energy balances yields a simple expression for gas temperature in the receiver:

$$T = \gamma T_o - \left[\frac{\gamma T_o - T_i}{1 + \frac{\dot{m}_o}{M_i}t}\right] \rightarrow \gamma T_o \tag{45}$$

Equation 45 shows that the absolute temperature in the downstream receiver will ultimately reach 356 C (γT_o) as mass continues to be introduced into the vessel. The pressure will continue to increase linearly with time as mass continues to increase and as the temperature reaches γT_o:

$$\frac{dP}{dt} = \frac{R_g \dot{m}_o}{M_w V}\gamma T_o = \frac{\dot{m}_o}{V}H_o\left(\gamma - 1\right) \tag{46}$$

$$\frac{dP}{dM} = \frac{1}{V}H_o\left(\gamma - 1\right) \tag{47}$$

Figure 1: SuperChems Expert prediction of pressure during vessel charging using non-ideal gas behavior

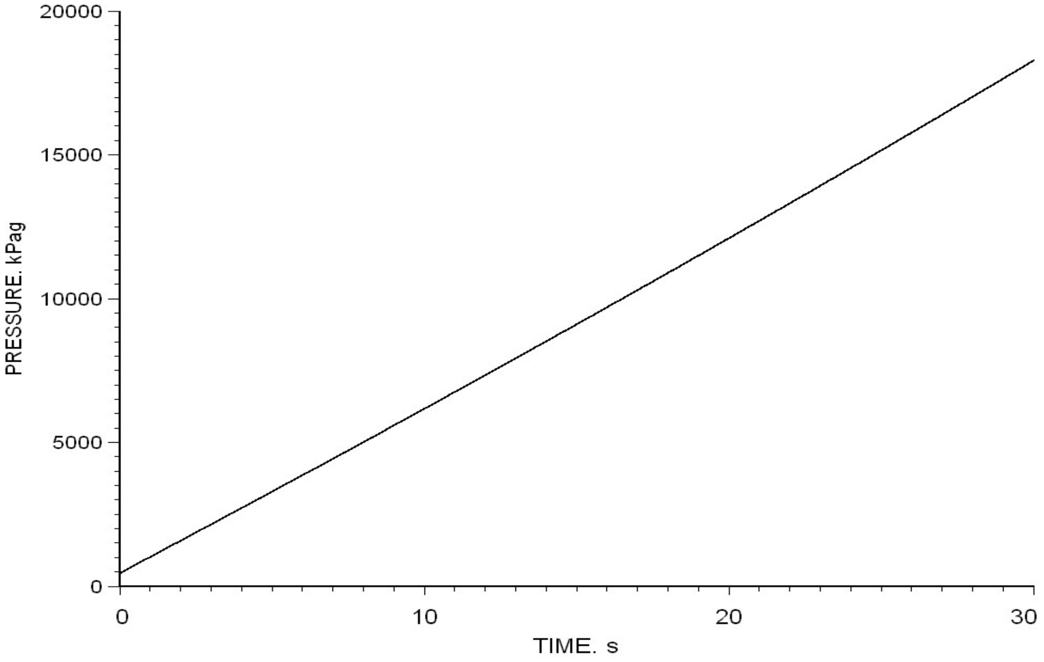

The dynamics of vessel charging for this example are calculated using SuperChems Expert v7.23. The temperature and pressure histories are illustrated in Figures 1 and 2 using real gas behavior. The numerical solution confirms the temperature and pressure analytical predictions using the ideal gas behavior.

The subject of vessel charging has been discussed in the literature [8, 9] to determine maximum fluid and wall temperatures during rapid filling. This can be important during rapid filling of natural gas cylinders for natural gas powered vehicles [10]. In addition, SuperChems Expert™ allows the user to perform the same simulation while enabling heat heat exchange between the receiver contents and walls/surroundings. Modeling of the heat exchange yields better estimates of peak fluid temperatures and wall segment temperatures when the charging rate is slow enough.

7 Pressure Relief Systems Considerations

If we consider the actual case of gas blow through from the 10 m^3 high pressure separator into the smaller volume of 1.93 m^3, the flow rate into the small receiver will remain constant until the receiver pressure reaches the upstream choke pressure, approximately 2114 kPag. Once that pressure is reached in the receiver, the flow will become subsonic, and the pressures will ultimately equalize in both vessels.

The assumption of negligible heat transfer to/from the surroundings is a reasonable assumption [11] if the flow duration is short because the natural convection heat transfer coefficient from the inner vessel wall to the fluid is small. These dynamics were calculated using SuperChems Expert and

Figure 2: SuperChems Expert prediction of temperature during vessel charging using non-ideal gas behavior

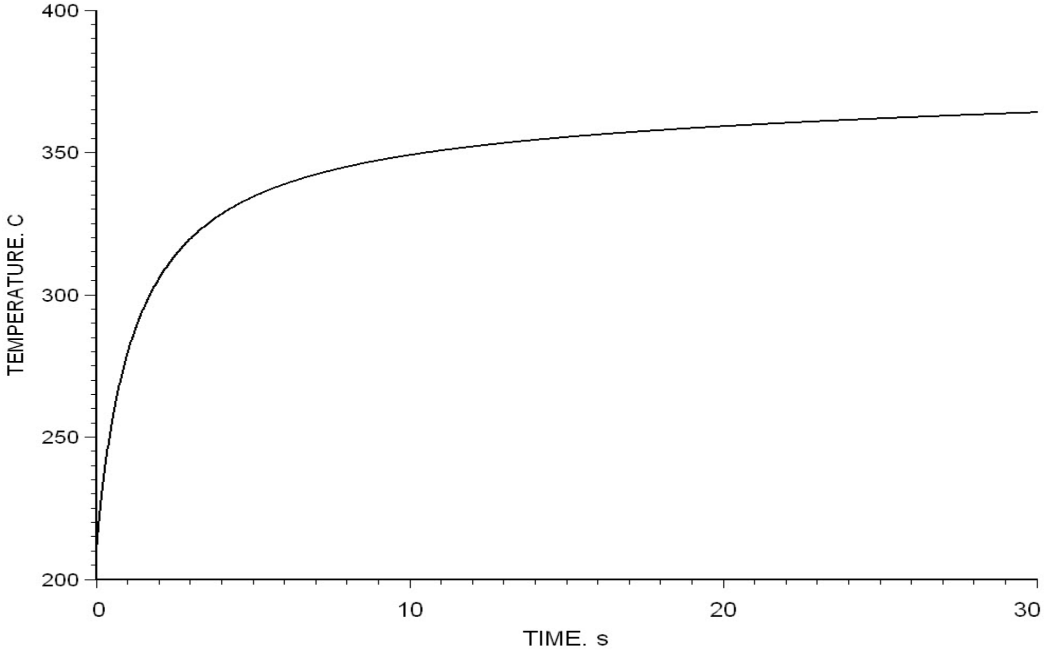

are illustrated in Figure 3 and Figure 4 .

Typically, the downstream receiver vessel will be outfitted with a pressure relief device to protect from overpressure. For vessels containing two phases downstream of the high pressure gas source, the initial steady state vapor space composition can be substantially different from the gas composition of the incoming gas due to the presence of two phases in the vessel. Sizing of the pressure relief device should take into account the rapid compression of the vapor space up to the full open pressure of the pressure relief device as well as the molecular weight of the resulting gas mixture which can be different from that of the incoming high pressure gas. If the superficial vapor velocity is high enough, two-phase flow can result [12].

8 Temperature Increase Caused by Bubble Compression

Shocks created by the rapid introduction of a high pressure fluid into a low pressure fluid can cause gas bubble compression and/or spontaneous bubble collapse. This can lead to elevated temperatures or hot spots in the gas bubble as well as for the gas/liquid or gas/solid interface for multiphase systems.

Gas bubbles (voids) can have a significant impact on the maximum pressure and temperature reached in a medium under shock. Waxes and polymers with suspended voids are often used as binders for high explosives to reduce (or enhance) their sensitivity. It is well known that the sensitivity of high explosives can be reduced by wax or polymer binders (5-10 % of a binder in an explosive composition). The sensitivity of high explosives with binders can be further reduced

Figure 3: SuperChems Expert Venting dynamics from high pressure separator into low pressure receiver - Pressure

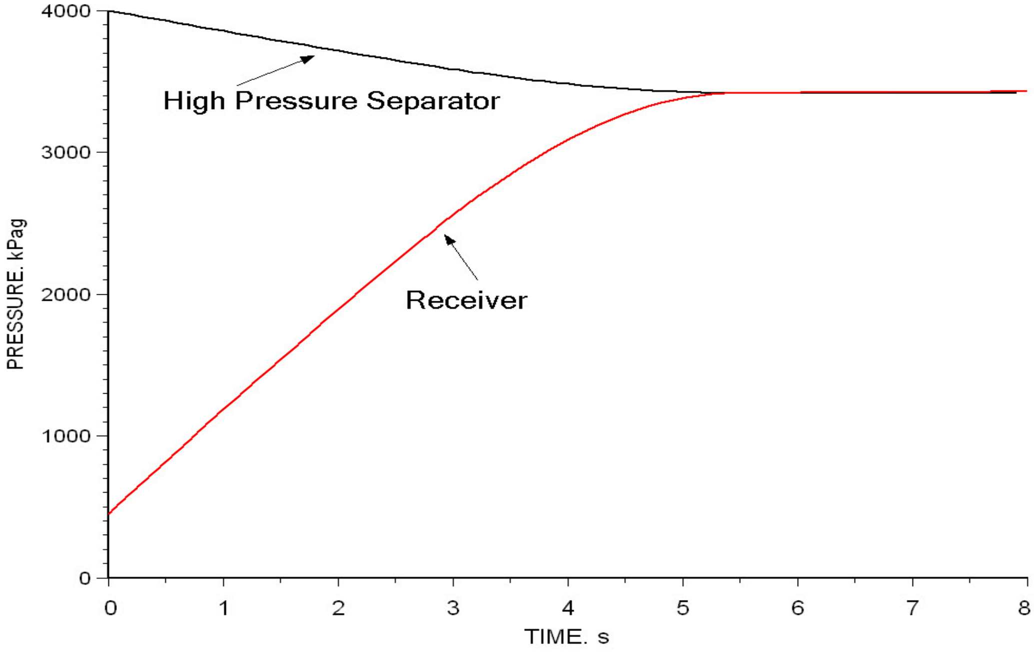

Figure 4: SuperChems Expert Venting dynamics from high pressure separator into low pressure receiver - Temperature

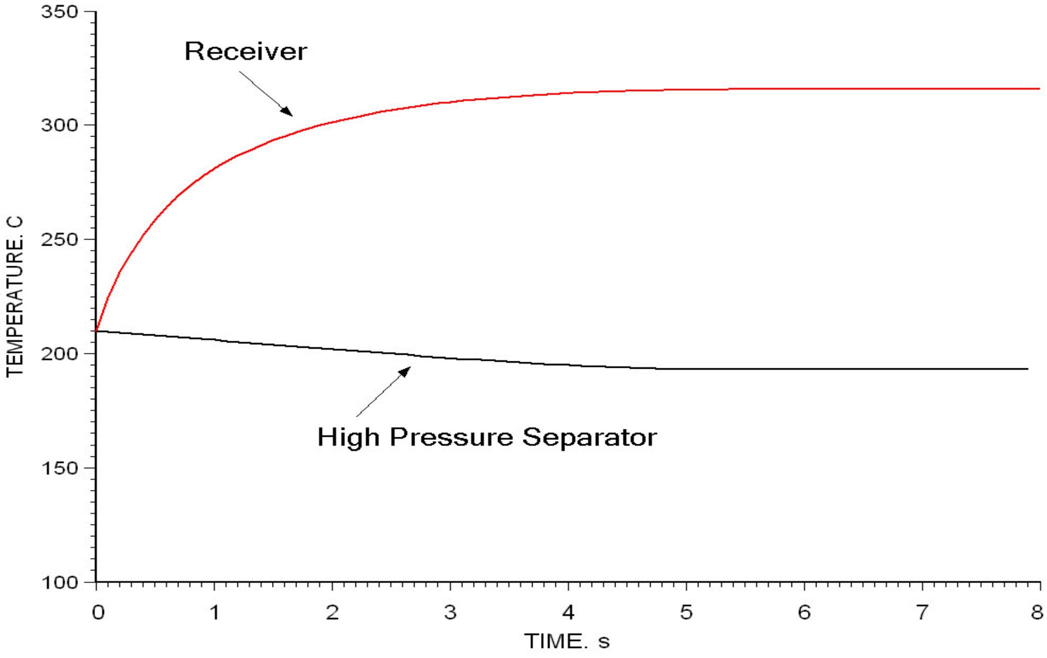

if the voids added are filled with a specific gas as shown later in this section. Voids can make explosives more sensitive to impact. However, some materials with voids (i.e. porous materials, foams and bubbly liquids) can damp pressure waves drastically. Inclusion of such materials could prevent shock-to-detonation transitions and reduce the sensitivity of high explosives and certain shock sensitive solids and reactive liquids. It is possible that small amounts of very carefully designed porous additives could substantially reduce the sensitivity of standard high explosives or sensitive liquid and/or solid compounds.

First, when compressed, voids heat up. At high compression they can drive temperature of interfaces up to melting points or ignition/runaway temperatures for chemical reactions. The heat transfer both in gaseous and condensed phases reduces the temperatures. The balance between adiabatic heating and heat losses determines the temperatures at the interface. This balance depends on void sizes and shapes and can be controlled by proper selection of void sizes. Another important effect is the value of the adiabatic compression factor of the gas. For 'heavy' gases with adiabatic compression factors near unity, the pressure changes lead to small changes of temperature.

Second, the pressure field around a single void is determined by non-linearity, dispersion, dissipation and relaxation of the multiphase medium. These properties depend on void fraction, void sizes, rheology of condensed material, and even on the gas inside the bubble (e.g., theoretical and experimental studies of pressure waves in bubbly liquids show that shock waves attenuate faster in liquids with helium bubbles, rather than with air bubbles).

In some situations, the complex structure of the medium can amplify pressure waves, in others a considerable dissipation of waves takes place. Voids can significantly influence pressure waves in liquids at low relative void fraction of bubbles (0.01 - 1 %).

The characteristic feature of problems connected with wave dynamics in a multiphase medium is a large space of dimensionless parameters governing the process (in standard models we have 10-20 dimensionless numbers). Although, it is challenging to find and optimize the parameters of the medium to get desirable properties (e.g. highest threshold for shock-to-detonation transition), the medium can be controlled by changing some specific parameters. Thus, explosive binders and reactive liquids with desirable sensitivity to shocks can be designed.

When a shock wave propagates through liquids with bubbles, the temperature inside the bubbles increases adiabatically, while the temperature in the bulk liquid remains constant. Kinetics of chemical reactions taking place in the liquid phase depend on the temperature of liquid, not the gas. That is why it is important to be able to estimate the maximum possible temperature in the liquid phase following a shock, which is lower than the adiabatic compression temperature in the gas.

Let us consider that T_0 is the temperature of liquid far from the bubble, and P_0 is the undisturbed pressure. The adiabatic temperature (T_g) at the center of the bubble under compression could be found by the relation:

$$T_g = T_0 \left(\frac{P_g}{P_0} \right)^{\frac{\gamma-1}{\gamma}} \tag{48}$$

where P_g is the gas pressure and γ is the gas adiabatic compression coefficient. In the absence of phase transitions, heat fluxes in the gas and liquid are equal at the interface ($q_g = q_l$):

$$q_g = \lambda_g \frac{T_g - T_i}{\delta_g} \tag{49}$$

$$q_l = \lambda_l \frac{T_i - T_0}{\delta_l} \tag{50}$$

$$\delta_g = \sqrt{k_g t} \tag{51}$$

$$\delta_l = \sqrt{k_l t} \tag{52}$$

Where λ, k, and δ are the thermal conductivity and diffusivity, and the thickness of thermal boundary layer, T_i is the temperature of the interface and t is time.

Using the heat balance equation and relation 48 and the equations above we can find the following expression for the interface temperature:

$$T_i = T_0 \frac{1 + k \left(\frac{P_g}{P_0}\right)^{\frac{\gamma-1}{\gamma}}}{1+k} \tag{53}$$

$$k = \frac{\lambda_g}{\lambda_l}\sqrt{\frac{k_l}{k_g}} \tag{54}$$

The thermal conductivity and diffusivity of gas depends on temperature and pressure. For ideal gases with linear dependence of the thermal conductivity on gas temperature, k depends only on pressure:

$$k = k_0 \sqrt{\frac{P_g}{P_0}} \tag{55}$$

$$\frac{\lambda_g}{\sqrt{k_g}} = \sqrt{\lambda_g \rho_g c_g} = \sqrt{\frac{\lambda_{g,0} c_g}{T_0 R_g}\left(\rho_g R_g T_g\right)} = \sqrt{\frac{\lambda_{g,0} c_g}{T_0 R_g} P_g} \sim \sqrt{P_g} \tag{56}$$

Note that here we assume the spatial homogeneity of the gas pressure. This assumption holds as long as the velocity of decreasing bubble radius is much less than the speed of sound in the gas. Therefore, the final expression for the interface temperature can be rewritten in the form:

$$T_i = T_0 \frac{1 + k_0 \left(\frac{P_g}{P_0}\right)^{\frac{3}{2} - \frac{1}{\gamma}}}{1 + k_0 \left(\frac{P_g}{P_0}\right)^{\frac{1}{2}}} \tag{57}$$

Table 2: The Interface Temperature (C) Driven at Adiabatic Bubble Compressions

Gas	γ	k_0	$\frac{P_g}{P_0} = 1$	$\frac{P_g}{P_0} = 10$	$\frac{P_g}{P_0} = 100$	$\frac{P_g}{P_0} = 1000$
Helium	1.67	0.00711	20	30	123	819
Air	1.4	0.00351	20	23	47	201
Carbon Dioxide	1.29	0.00314	20	22	36	119
Sulfur Hexafluoride	1.095	0.00456	20	21	26	50

where

$$k_0 = \frac{\lambda_{g,0}}{\lambda_l}\sqrt{\frac{k_l}{k_{g,0}}} \tag{58}$$

The subscript zero denotes the undisturbed state. Table 2 provides sample data calculated by using Equation 57 when the parameters of undisturbed liquid are the same as for water at ambient temperature and pressure.

Table 2 shows that at high compressions the type of gas in the bubbles has a significant impact on the maximum temperature in the liquid, mainly because of the difference in the gas adiabatic exponent.

9 Compression Ignition

A section of an ethylene pipeline at 1500 psig was taken out of service for cleaning/maintenance. The repaired section was purged with nitrogen prior to re-introduction of ethylene. Some time later, the pipeline ruptured a few hundred yards from the repaired section, and flames shot out several hundred feet into the air. What happened can be attributed to what is called ”compression ignition”. In this case, the compression caused the decomposition of ethylene.

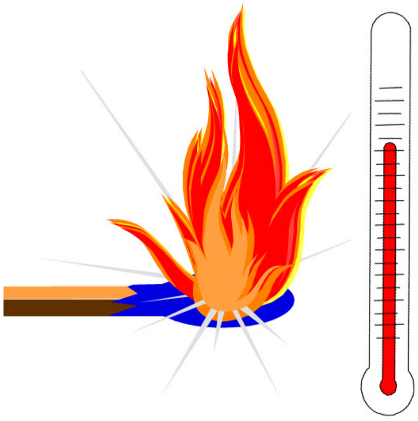

Nitrogen was compressed by the rapid introduction of high pressure ethylene ($\simeq$100:1 ratio). The compression raised the temperature of the ethylene and nitrogen to the decomposition temperature of ethylene. The ethylene decomposition flame propagated slowly along the pipe until it met the main flow. The flame stabilized at that point and heated the pipe wall to a temperature sufficient to weaken and rupture the pipe.

This incident could have been avoided by slowly re-introducing the ethylene to prevent compression heating and to allow for heat exchange between the two fluids and the

Table 3: Compressed Temperature as a function of pressure

Gas	γ	$\frac{P_f}{P_0} = 5$	$\frac{P_f}{P_0} = 20$	$\frac{P_f}{P_0} = 50$	$\frac{P_f}{P_0} = 100$
Air	1.4	199	429	639	838
Isobutane	1.1	77	120	166	197

pipe wall and surroundings. A flame arrester could have also prevented the propagation of the decomposition flame [13].

The compressed gas temperature can easily be estimated using ideal gas behavior or by using computational tools like SuperChems Expert to account for the non-ideal behavior of the fluids and all the heat exchange mechanisms. Assuming ideal behavior and adiabatic (isentropic) compression, the final compressed gas temperature becomes:

$$T_f = T_0 \left(\frac{P_f}{P_0} \right)^{\frac{\gamma - 1}{\gamma}} \tag{59}$$

Table 3 illustrates typical compressed temperature values for air and isobutane. We note that the autoignition temperature for most hydrocarbons is less than 530 °C.

Compression ignition hazards can be minimized. Special care is recommended where inert gas compression is possible with ethylene service. Flammable vapors should be kept out of compressor intakes and air should be kept out of hydrocarbon vapors compressors. High pressure oxygen systems require special care.

10 Conclusions

We have demonstrated through fundamentals that rapid charging of an ideal gas closed system can result in an elevated temperature that asymptotes towards γT_o where T_o is the temperature of the incoming gas.

SuperChems Expert is a very useful and reliable dynamic simulation software that can provide insight into compression heating for simple and complex systems with chemical reactions and/or non-ideal behavior. SuperChems Expert can be used to establish the optimal relief requirement for specific charging duration with consideration of vapor/liquid disengagement and multiphase reacting flows. In addition, the vessels can be divided into multiple segments and wall temperatures can be estimated for each segment for proper selection of materials of construction.

A Appendix A - Volume Change for Piping and Vessels ($\frac{dV_s}{dt}$)

The volume of a solid, just like a fluid, expands and contracts due to changes in temperature and pressure. Because the change in volume for solids is smaller than the volume change for liquids and gases, it is normally neglected in most fluid flow applications. There are some practical applications where the volume change of a pipe or vessel can be important when considering scenarios dealing with loss of containment. Thermal expansion of liquid full vessels and/or piping is one such application. The depressuring of long high pressure pipelines is another practical application.

For vessels or piping containing liquids or vapors that are subjected to heating, the overall change of vessel volume due to thermal expansion and increase in internal pressure as a function of time is given by:

$$\frac{dV_s}{dt} = \left[\frac{\partial V_s}{\partial T}\right]_P \frac{dT}{dt} + \left[\frac{\partial V_s}{\partial P}\right]_T \frac{dP}{dt} = 3\alpha_s V_s \frac{dT}{dt} + \left(\frac{D_i}{\delta}\right)\left(\frac{V_s}{E_{s,T}}\right) f(\nu)\frac{dP}{dt} \tag{60}$$

where α_s is the material of construction coefficient of thermal linear expansion, $E_{s,T}$ is the material of construction modulus of elasticity (see Figure 5), D_i is the internal vessel diameter, δ is the vessel wall thickness, ν is Poisson's ratio, and $f(\nu)$ depends on the vessel geometry:

$$f(\nu) = 1.25 - \nu \simeq 0.95 \quad \text{for a cylindrical vessel, and} \tag{61}$$

$$f(\nu) = \frac{3}{4}(1-\nu) \simeq 0.53 \quad \text{for spherical vessel.} \tag{62}$$

A.1 Change of Volume with Respect to Temperature

Unlike liquids and gases, the change of volume of a solid due to a change in temperature is typically calculated from the solid linear expansion coefficient, α_s:

$$\frac{\partial L}{\partial T} = \alpha_s(T)L \tag{63}$$

where L is the length of the solid, T is the temperature, and α_s is the coefficient of linear thermal expansion typically expressed in units of $\frac{\text{m}}{\text{m.K}}$. It can be shown that thermal expansion of a solid in 2D (area) or 3D (volume) can be related to the linear coefficient of thermal expansion [2]:

$$\frac{\partial A_s}{\partial T} = 2\alpha_s(T)A_s \tag{64}$$

$$\frac{\partial V_s}{\partial T} \simeq 3\alpha_s(T)V_s \tag{65}$$

---

[2] For example, for a cylinder, $V_s = \frac{\pi D^2}{4}L$. Differentiating V_s with respect to temperature yields $\frac{\partial V_s}{\partial T} = \frac{\pi}{4}\left[D^2\alpha_s L + 2\alpha_s L D^2\right] = 3\alpha_s\frac{\pi D^2}{4}L = 3\alpha_s V_s$

Figure 5: Temperature dependency of modulus of elasticity for some common materials of construction [1]

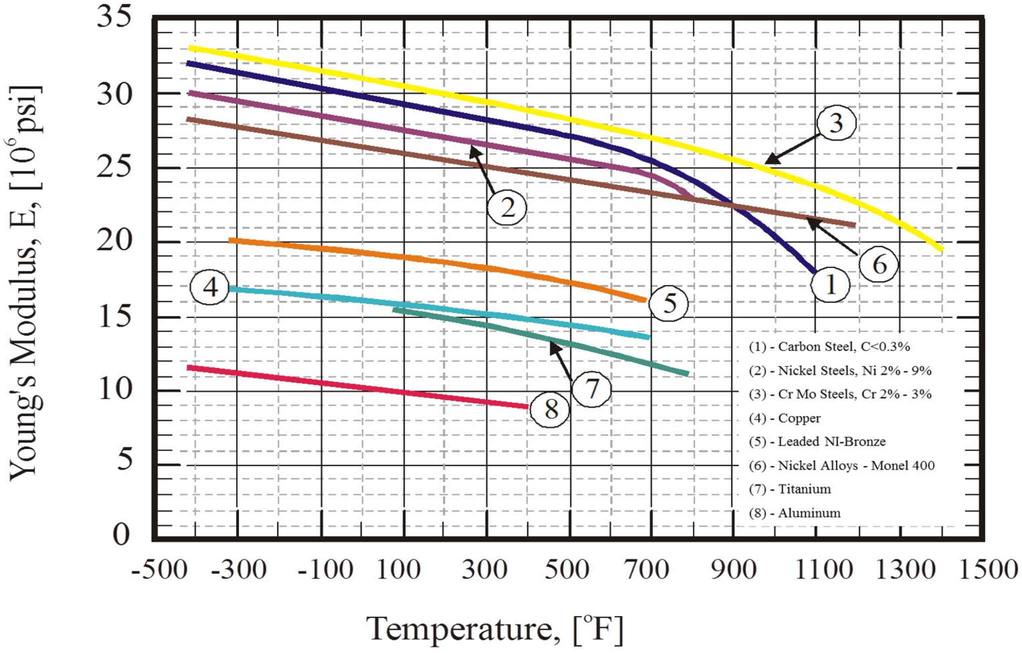

Typical values of α_s are shown in Table 4 for some common metals and materials of construction. As shown by Table 4, liquid thermal expansion is much larger than steel thermal expansion and almost all the liquid thermal expansion will contribute to stressing the liquid full pipe or vessel. α_s is a weak function of temperature.

A.2 Change of Volume with Respect to Pressure

The change of a solid volume with respect to pressure can be related to the isothermal compressibility of the solid. The isothermal compressibility, κ, is not used for solids. Instead, the bulk modulus of elasticity is typically used:

$$\kappa = -\frac{1}{V}\left[\frac{\partial V}{\partial P}\right]_T = \frac{1}{\rho}\left[\frac{\partial \rho}{\partial P}\right]_T = \frac{1}{E_T} \tag{66}$$

For thin walled ($\frac{D_i}{\delta} > 10$), hollow piping and vessels, the change of volume with respect to pressure is proportional to the isothermal compressibility and diameter to thickness ratio:

$$\frac{\partial V_s}{\partial P} = \left(\frac{D_i}{\delta}\right)\left(\frac{V_s}{E_{s,T}}\right)[1.25-\nu] \quad \text{Cylinder} \tag{67}$$

$$\frac{\partial V_s}{\partial P} = \left(\frac{D_i}{\delta}\right)\left(\frac{V_s}{E_{s,T}}\right)\left[\frac{3}{4}(1-\nu)\right] \quad \text{Sphere} \tag{68}$$

Table 4: Coefficient of linear thermal expansion for some common metals and materials of construction at 293.15 K

Solid	$\alpha_s \times 10^6$, m/m/K	$3\alpha_s \times 10^6$, m/m/K
Aluminum	25	75
Brass	19	56
Copper	17	51
Gold	14	42
Steel	12	35
Invar (Nickel-Iron Alloy)	0.9	2.7
Lead	29	87
Silver	18	54
Glass (typical)	9	27
Glass (Pyrex)	3	9
Quartz	0.4	1
Concrete, Brick	$\simeq 12$	$\simeq 36$
Marble (typical)	2.5	7.5
Water		210
Air		3400

where ν is Poisson's ratio [3] which is approximately equal to 0.3 for steel.

A.3 Volume Change for Fluids

The excess volume change of a liquid / gas mixture contained in an elastic vessel/pipe caused by a change in temperature and/or pressure is given by:

$$\frac{dV_{excess}}{dt} = (V_v\beta_v + V_l\beta_l)\frac{dT}{dt} - (V_v\kappa_v + V_l\kappa_l)\frac{dP}{dt} + \sum_i \overline{V}_{v_i}\frac{dN_i}{dt} + \sum_i \overline{V}_{l_i}\frac{dn_i}{dt} - \frac{dV_s}{dt} \tag{69}$$

where κ is the isothermal compressibility and β is the volume expansion coefficient. κ and β are typically calculated from an equation of state.

Excess volumetric change due to thermal expansion would have to be provided by the relief device in order to keep the pressure from exceeding a limiting value. If we assume the piping or vessel containing the fluid mixture is rigid, i.e. $\frac{dV_s}{dt} = 0$ then:

$$\frac{dV_{excess}}{dt} = (V_v\beta_v + V_l\beta_l)\frac{dT}{dt} - (V_v\kappa_v + V_l\kappa_l)\frac{dP}{dt} + \sum_i \overline{V}_{v_i}\frac{dN_i}{dt} + \sum_i \overline{V}_{l_i}\frac{dn_i}{dt} \tag{70}$$

---

[3] Ratio of strain in a traverse direction to that in the longitudinal direction, $\nu = \frac{\epsilon_{lateral}}{\epsilon_{axial}} = \frac{\frac{\Delta D}{D}}{\frac{\Delta L}{L}}$ where ϵ is the strain in m/m or in/in.

If we also assume the piping and/or vessel is full of a single phase fluid with a negligible partial molar volume we can write:

$$\frac{dV_{excess}}{dt} = (V\beta)\frac{dT}{dt} - (V\kappa)\frac{dP}{dt} \tag{71}$$

B Appendix B - Ideal Nozzle Flow Rates

B.1 Liquids

Liquid ideal nozzle flow can be calculated using the following simple expression, adjusted for subcooled and non-equilibrium flow:

$$\dot{m} = \rho_l A_h C_d u = \rho_l A_h C_d \underbrace{\sqrt{\frac{2}{\rho_l}\left[P - (1-C)\,P_s\right]}}_{u} = A_h C_d \sqrt{2\rho_l \left[P - (1-C)\,P_s\right]} \tag{72}$$

$$\tag{73}$$

where P_s is the larger of ambient pressure or the bubble point pressure of the liquid at the current temperature.

Burnell [14] used the bubble delay factor, C, to approximate the impact of non-equilibrium on mass flow. C is directly related to the bubble growth delay time and typically ranges from 0.2 to 0.3. The magnitude of C determines the pressure undershoot at the choke point/exit due to the superheating of the liquid. C tends to 0 as the starting initial temperature approaches the critical temperature. Depending on the flow conditions, C can also depend on the length of pipe and initial vapor quality. For pipe flow, it has long been recognized that a pipe flow length of approximately 4 inches [15] is required for equilibrium two-phase flow to develop, $C = 0$. Non-equilibrium is most important for nozzle flow (PRV flow) and for short piping (also see [16, 17, 18]).

B.2 Ideal Gases

For ideal gas flow, $\dot{m}$ can be calculated from the following equation assuming that the incoming upstream fluid velocity is zero:

$$\dot{m} = C_d A_h \sqrt{2P\rho\left(\frac{\gamma}{\gamma-1}\right)\left[\left(\frac{P_e}{P}\right)^{2/\gamma} - \left(\frac{P_e}{P}\right)^{\frac{\gamma+1}{\gamma}}\right]} \tag{74}$$

where $P_e = P_c$ if P_c is greater than the ambient back pressure, P_s:

$$P_e = P_c = P\left(\frac{2}{\gamma+1}\right)^{\frac{\gamma}{\gamma-1}} \geq P_s \tag{75}$$

P_c is the critical flow pressure. Under these conditions the mass flux is not influenced by the ambient back pressure up to P_c and the flow is said to be choked or sonic. Under choked flow conditions, the mass flow rate can be calculated from a simplified form of the above equation which incorporates the critical pressure ratio P_c from Equation 75:

$$\dot{m} = C_d A_h \sqrt{\gamma P \rho \left(\frac{2}{\gamma+1}\right)^{\frac{\gamma+1}{\gamma-1}}} \tag{76}$$

For subsonic flow, P_e is equal to P_s, and the mass flow is calculated from Equation 74.

References

[1] M. A. Grolmes. Odds and ends - relief valve stability - Part 4. In *DIERS Users Group Meeting*. American Society of Chemical Engineers, AIChE/DIERS, 2011.

[2] G. A. Melhem, R. Saini, and B. M. Goodwin. A modified Peng-Robinson equation of state. *Fluid Phase Equilibria*, 47:189–237, 1989.

[3] G. A. Melhem, R. Saini, and C. F. Leibovici. On the application of concentration dependent mixing rules to systems containing large numbers of compounds. In *2nd International Symposium of SuperCritical Fluids*, pages 475–477, May 1991.

[4] G. A. Melhem, H. G. Fisher, and D. A. Shaw. An advanced method for the estimation of reaction kinetics, scale-up and pressure relief design. *Process Safety Progress*, 14(1):1–21, 1995.

[5] G. A. Melhem and D. Gaydos. Properly calculate vessel and piping wall temepratures during depressuring and relief. *Process Safety Progress*, 34(1):64–71, 2015.

[6] G. A. Melhem. Proper calculations of pipe and vessel wall temperatures during relief and/or depressurization. In *78th API Fall Refining and Equipment Standards Meeting*, pages 221–226, November 2013.

[7] M. L. Michelsen. An efficient general purpose method for the integration of stiff ordinary differential equations. *AIChE Journal*, 22(3):594–597, 1976.

[8] Frederick J. Moody. *Introduction to Unsteady Thermofluid Mechanics*. Wiley, 1990.

[9] J. Craig Dutton and Robert E. Coverdill. Experiments to study the gaseous discharge and filling of vessels. *International Journal of Engineering Eduction*, 13(2):123–134, 1997.

[10] Mahmood Farzaneh-Gord. Real and ideal gas thermodynamic analysis of single reservoir filling process of natural gas vehical cylinders. *Journal of Theoretical and Applied Mechanics*, 41(2):21–36, 2011.

[11] W. S. Winters, G. H. Evans, S. F. Rice, and R. Greif. An experimental and theoretical study of heat and mass transfer during the venting of gas from pressure vessels. *International Journal of Heat and Mass Transfer*, 55:8–18, 2012.

[12] G. A. Melhem. Two-phase flow onset and disengagement methods. *ioMosaic Corporation White Paper*, Novemeber 2020.

[13] G. A. Melhem. How flame arresters work. *ioMosaic Corporation White Paper*, October 2019.

[14] J. G. Burnell. Flow of boiling water through nozzles, orifices, and pipes. *Engineering Lond.*, 164:572, 1947.

[15] B. Fletcher. Flashing through orifices and pipes. AIChE Loss Prevention Symposium in Denver, 1983.

[16] G. A. Melhem. Retrograde and phase change (RPC) flow considerations for relief and flare systems. *ioMosaic Corporation White Paper*, 2018.

[17] G. A. Melhem. Retrograde and phase change (RPC) flow considerations for relief and depressuring systems. *ioMosaic Corporation White Paper*, 2018.

[18] G. A. Melhem. Non-equilibrium flow and rapid phase transitions (RPT). In *DIERS Spring Virtual Meeting*. AIChE, March 2021.

Index

Chemical reactivity, 28

Dust, 28

ethylene, 5

Flammability, 28

ioKinetic® , 28
ioMosaic® , 27, 28
ISO certified, 28

About the Authors

Dr. Melhem is an internationally known pressure relief and flare systems, chemical reaction systems, process safety, and risk analysis expert. In this regard he has provided consulting, design services, expert testimony, incident investigation, and incident reconstruction for a large number of clients. Since 1988, he has conducted and participated in numerous studies focused on the risks associated with process industries fixed facilities, facility siting, business interruption, and transportation.

Prior to founding ioMosaic® Corporation, Dr. Melhem was president of Pyxsys Corporation; a technology subsidiary of Arthur D. Little Inc. Prior to Pyxsys and during his twelve years tenure at Arthur D. Little, Dr. Melhem was a vice president of Arthur D. Little and managing director of its Global Safety and Risk Management Practice and Process Safety and Reaction Engineering Laboratories.

Dr. Melhem holds a Ph.D. and an M.S. in Chemical Engineering, as well as a B.S. in Chemical Engineering with a minor in Industrial Engineering, all from Northeastern University. In addition, he has completed executive training in the areas of Finance and Strategic Sales Management at the Harvard Business School. Dr. Melhem is a Fellow of the American Institute of Chemical Engineers (AIChE) and Vice Chair of the AIChE Design Institute for Emergency Relief Systems (DiERS).

Contact Information

Georges. A. Melhem, Ph.D., FAIChE
E-mail. melhem@iomosaic.com

ioMosaic Corporation
93 Stiles Road
Salem, New Hampshire 03079
Tel. 603.893.7009, x 1001
Fax. 603.251.8384
web. www.iomosaic.com

How can we help?

Please visit www.iomosaic.com and www.iokinetic.com to preview numerous publications on process safety management, chemical reactivity and dust hazards characterization, safety moments, video papers, software solutions, and online training.

In addition to our deep experience in process safety management (PSM), chemical reaction systems, and the conduct of large-scale site wide relief systems evaluations by both static and dynamic methods, we understand the many non-technical and subtle aspects of regulatory compliance and legal requirements. When you work with ioMosaic® you have a trusted ISO certified partner that you can rely on for assistance and support with the lifecycle costs of relief systems to achieve optimal risk reduction and PSM compliance that you can evergreen. We invite you to connect the dots with ioMosaic®.

We also offer laboratory testing services through ioKinetic® for the characterization of chemical reactivity and dust/flammability hazards. ioKinetic® is an ISO accredited, ultramodern testing facility that can assist in minimizing operational risks. Our experienced professionals will help you define what you need, conduct the testing, interpret the data, and conduct detailed analysis. All with the goal of helping you identify your hazards, define and control your risk.

ioMosaic®
Minimizing risk. Maximizing potential.®

About ioMosaic Corporation

Our mission is to help you protect your people, plant, stakeholder value, and our planet.

Through innovation and dedication to continual improvement, ioMosaic has become a leading provider of integrated process safety and risk management solutions. ioMosaic has expertise in a wide variety of disciplines, including pressure relief systems design, process safety management, expert litigation support, laboratory services, training, and software development.

As a certified ISO 9001:2015 Quality Management System (QMS) company, ioMosaic offers integrated process safety and risk management services to help you manage and reduce episodic risk. Because when safety, efficiency, and compliance are improved, you can sleep better at night. Our extensive expertise allows us the flexibility, resources, and capabilities to determine what you need to reduce and manage episodic risk, maintain compliance, and prevent injuries and catastrophic incidents.

Consulting Services

- Asset Integrity
- Auditing
- Due Diligence
- Facility Siting
- Fault Tree/SIL Analysis
- Fire & Explosion Dynamics
- Incident Investigation, Litigation Support, and Expert Testimony
- Hydrogen Safety
- LNG Safety
- LPG Safety
- Pipeline Safety
- Process Hazard Analysis
- Process Engineering Design and Support
- Process Safety Management
- Relief and Flare Systems Design and Evaluation
- Risk Management Program Development
- Quantitative Risk Assessment
- Software Solutions
- Structural Dynamics
- Sustainability Reporting Support
- Technology Transfer Package Development
- Process Safety Training

US Offices

Salem, New Hampshire
Houston, Texas
Minneapolis, Minnesota
Berkeley, California

International Offices

Al Seef, Kingdom of Bahrain
Bath, United Kingdom

Software Solutions

Process Safety Office® : A suite of integrated tools for process safety professionals and risk analysts.

Process Safety Enterprise® : Process Safety Management compliance made easy with enterprise workflows, dynamic forms, document management, key performance indicators and metrics, and more.

Process Safety Learning® : Build your process safety competencies incrementally using learning modules.

Process Safety tv® : The worldś first video streaming platform dedicated to process safety.

Contact us

www.ioMosaic.com
sales@ioMosaic.com
1.844.ioMosaic

Laboratory Testing Services (ISO Accredited)

- Battery Safety Testing
- Chemical Reactivity Testing
- Combustible Dust Hazard Analysis and Testing
- Flammability Testing
- Physical Properties Testing
- Process Safety Services
- Specialized Testing